

HIGHLIGHTS OF UWB IMPULSE BEAMFORMING

Sigmar Ries¹ and Thomas Kaiser²

1: Fachhochschule Südwestfalen
Dept. Meschede
Lindenstr. 53, D-59872 Meschede
Germany
email: ries@fh-swf.de

2: Duisburg-Essen University
Faculty of Engineering
Department of Communication Systems
Bismarckstraße 81, 47048 Duisburg, Germany
email: thomas.kaiser@uni-duisburg.de

ABSTRACT

In this paper, general results for ideal UWB (Ultrawideband) impulse beampattern are given. It can be easily shown that the mainlobe width is similar to the narrowband case. In contrast, the absence of grating lobes and the appearance of a fixed sidelobe level dependent only on the number of antennas and *not* on their spacing is a beneficial property. A further unusual fact is that unequal prefiltering or weighting of the array antennas leads to an *increase* of the sidelobe level. Numerical simulations validate these unfamiliar results. In conclusion, the design of UWB arrays needs special attention.

1. INTRODUCTION

Beamforming for UWB impulse signals shows some special features, and some of them are different from the narrowband case. Also, there are several possible definitions of the *beampattern*; we will present 3 cases and investigate one of them in more detail. First, a coarse estimate of the mainlobe width shows that this parameter is similar to the usual narrowband case. Second, the investigation of ideal time-delay beamforming for short pulses exhibit a striking feature, namely the absence of grating lobes in the beampattern. This means that the spacing of the array elements is not limited by half of the wavelength, hence high resolution can be achieved with only a few array elements. A further surprising property is that the use of unequal prefilters or weighting for the individual antennas is detrimental for the sidelobe level, which is in clear contrast to the narrowband case. Although these results are valid in a rather general broadband setting, we will give simulation results for the special case of UWB impulse beamforming.

2. IDEAL BEAMFORMING FOR UWB PULSES

To start with, we consider the case of a linear equispaced array, consisting of N equidistant omnidirectional antennas. If c is the propagation speed, θ the angle of incidence of a time-limited impulse signal $s(t)$ measured with respect to broad-side direction and d the distance between two sensors, then the signal recorded at the n -th sensor is given by

$$y_n(t) = s\left(t + n \frac{d}{c} \sin(\theta)\right) = s(t + n \tau), \quad n = 0(1)N-1,$$

where $\tau = (d/c) \sin(\theta)$. The ideal "delay and sum" or time-delay beamformer produces

$$y(\theta, t) = \frac{1}{h_n} \sum_{n=0}^{N-1} h_n y_n(t - n \tau),$$

where $\tau = (d/c) \sin(\theta)$ are the *steering delays*, θ the *steering angle* and h_n the weighting coefficients. In order to achieve a *time-independent* beampattern the total energy

$$\text{BP}_{\text{TE}}(\theta, t) = \left(\int_{-}^+ |y(\theta, t)|^2 dt \right)^{1/2} \quad (1)$$

of the beamformer output has been proposed, as well as

$$\text{BP}_{\text{MAX}}(\theta, t) = \max_t |y(\theta, t)|, \quad (2)$$

see [3, 1, 6, 7] and the literature cited there. The formal advantage of (1) is to allow some meaningful analytical calculations; however, even for selected short broadband pulses, an exact closed form expression of (1) or (2) is not known so far. Also, the infinite integration time is unrealistic. For some special UWB pulses, approximate formulas for the beampattern have been developed [2].

In this paper, we propose an alternate definition of a time-invariant beampattern

$$\text{BP}(\theta, t) = \max_t \left(\int_{t-T/2}^{t+T/2} |y(\theta, t)|^2 dt \right)^{1/2}, \quad (3)$$

where the integration time T is matched to the duration of the UWB pulse. This is no drawback, since in all cases considered, the beampattern is dependent on the pulse shape. Also, this beampattern can be related to the impulse energy, which is a meaningful physical parameter. The beampattern given by this definition is not as convenient analytically tractable as (1), see [7] for details, but interesting general results can still be derived. It should be mentioned that all three beampattern definitions reduce to the usual narrowband beampattern in the case of narrowband signals.

3. MAJOR PROPERTIES OF THE BEAMPATTERN

3.1 Estimate of mainlobe width

In this section, we will give a coarse general but nevertheless quite precise estimate of the mainlobe width of the beampattern according to the definition (3). Let us assume that the impulse $s(t)$ is of finite duration T , the weighting coefficients are equal and the number of the array antennas is large. For simplicity an impulse coming from broadside is considered in the following. Based on these assumptions, known also from the narrowband case, the corresponding -3dB mainlobe angle θ_{-3dB} can be related to the arrays dimension and the impulse duration by [5]

$$\sin(\theta_{-3dB}) \approx \frac{2\sqrt{2}Tc}{L},$$

where L denotes the physical length of the array. This equation is "worst case" and can also be reformulated according to the classical narrowband setting. Note that for "simple" baseband pulses, bandwidth and duration are related by $B \approx 1/T$. If the bandwidth is taken to be 2 times some virtual center frequency f_c related to wavelength $\lambda_c = c/f_c$ we obtain, since the mainlobe is symmetric, the -3dB mainlobe width in the angular variable $u = \sin(\theta)$ as

$$\Delta u_{-3dB} \approx \sqrt{2} \frac{c}{L}.$$

This result is very similar to the narrowband case [8]; for concrete impulse shapes, the mainlobe width will certainly be smaller. This can be observed in the simulation results in section 4.

3.2 The sidelobe level for UWB impulse beamforming

We will first consider the grating lobes, which are well known in the narrowband case. It has already been mentioned in [2, 3, 6, 7], that there is an averaging effect for the UWB beampattern that mitigates grating lobes.

In the following the general case with a linear time-invariant prefilter $h_n(t)$ in each antenna branch yields

$$y(\theta, t) = \sum_{n=0}^{N-1} (s * h_n)(t + n \tau - n d \sin \theta),$$

where $*$ denotes convolution as usual [4]. Of course, the integration time T for the beampattern according to (3) has to be adapted to the maximum duration of the filtered pulse.

Note that in this way, a beamformer using matched filtering in each channel is included in our investigation by setting $h_n(t) = s(-t)^*$ for all n .

The following results can be stated [5]:

- If the duration of the pulse $s(t)$ and the filters $h_n(t)$ is limited by T_s and T_h , respectively, then for angles with

$$T_s + T_h < \frac{d}{c} \sin \theta, \quad (4)$$

the sidelobe level (SSL) for BP²(θ, t) is given by

$$SLL^2 = \max_t \left(\int_{t-T/2}^{t+T/2} \sum_{n=0}^{N-1} |(s * h_n)(t + n \tau - n d \sin \theta)|^2 dt \right). \quad (5)$$

- Further, the sidelobe level is bounded, and it holds

$$SLL^2 \leq \max_n 2 \left(\int_{t-T/2}^{t+T/2} |(s * h_n)(t)|^2 dt \right) = \max_n 2E_{s * h_n}. \quad (6)$$

For some special cases of practical importance, even more concrete information on the sidelobe level can be obtained:

- If the duration of the pulse $s(t)$ and the filters $h_n(t)$ is limited by T_s and T_h , then the following applies:

1. If

$$2(T_s + T_h) < \frac{d}{c} \sin \theta, \quad (7)$$

the fixed sidelobe level for BP²(θ, t) is given by

$$\begin{aligned} SLL^2 &= \max_n \int_{t-T/2}^{t+T/2} |(s * h_n)(t)|^2 dt \\ &= \max_n \int_{-}^{+} |(s * h_n)(t)|^2 dt = \max_n E_{s * h_n}. \end{aligned} \quad (8)$$

2. If all the prefilters h_n are equal and if

$$T_s + T_h < \frac{d}{c} \sin \theta, \quad (9)$$

the sidelobe level for BP²(θ, t) is given by

$$SLL^2 = \int_{-}^{+} |(s * h_1)(t)|^2 dt = E_{s * h_1}. \quad (10)$$

3. If instead of the prefilters simple weighting coefficients h_n are used, i. e. $h_n(t) = w_n(t)h_n$ and if

$$T_s < \frac{d}{c} \sin \theta, \quad (11)$$

then the sidelobe level is given by

$$SLL^2 = \max_n h_n \left(\int_{-}^{+} |s(t)|^2 dt \right) = E_s \max_n h_n. \quad (12)$$

- Thus in all cases, if the duration of the prefiltered pulses or pulses is short enough, and if steering angle and angle of incidence are sufficiently separated, a *fixed sidelobe level is accomplished* and its value is given by (5), (8), (10) or (12), respectively. The worst case is given by (5); but even then, the sidelobe level is at the maximum twice the fixed sidelobe level if $T_s + T_h < \frac{d}{c} \sin \theta$, as can be seen observed from (6).

As an example, in the case of equal prefilters and an angle of incidence of 90° , the fixed sidelobe level is reached at the steering angle of -90° if

$$T_s + T_h < \frac{2d}{c}.$$

If the pulse and/ or the filters have a shorter duration, the fixed level is achieved already at a smaller steering angle which can be computed from (11).

This means that for UWB impulse beamforming, there are virtually *no grating lobes*. In consequence, the spacing of the array elements is not limited by half of the wavelength, hence high resolution can be achieved with only a few array elements but sufficient spacing.

3.3 Ratio of mainlobe level to fixed sidelobe level

Without doubt this ratio is of interest for array design, because it is one of the key factors for the array's performance. We make the usual assumption that the maximum value of the beampattern shall occur for $\theta = 0$, i.e if the steering delays are matched to the impinging signal delays.

The maximum value of the beampattern can in this case be expressed as

$$BP^2(\theta, t) = \max_t \int_{t-T/2}^{t+T/2} \sum_{n=0}^{N-1} |(s * h_n)(t)|^2 dt.$$

Since $(s * h_n)(t)$ is duration-limited and the integration time T is equal to the maximum duration, the integration can be extended to $-\infty$ to $+\infty$, resulting in

$$\begin{aligned} BP^2(\theta, t) &= \int_{-\infty}^{+\infty} \sum_{n=0}^{N-1} |(s * h_n)(t)|^2 dt \\ &= \int_{-\infty}^{+\infty} |S(f)|^2 H_n(f) |df| \end{aligned}$$

where the second equation easily follows by Parsevals equation and the convolution theorem for Fourier transforms.

The main results of this paper are the following:

- The maximum ratio of mainlobe to fixed sidelobe level

$$\sqrt{\frac{BP^2(\theta, t)}{SLL^2}} \quad (13)$$

is N , and it is realized if and only if all the prefilters $h_n(t)$ are equal.

- Hence, for impulse beamforming an unequal prefiltering of the array elements is not only useless, but detrimental since it decreases the ratio of mainlobe to sidelobe level

Hence, impulse beamforming has a second feature that is opposite to the narrowband case, where unequal weighting or prefiltering is generally used to improve the ratio of mainlobe to sidelobe level or for interference cancellation. This result of course applies also to the special case of prefilters with single coefficients on behalf of filters. The proof for this case is given in appendix (2).

Since all prefilters are best chosen to be equal, they can be merged together after the adder, so that only one filter remains.

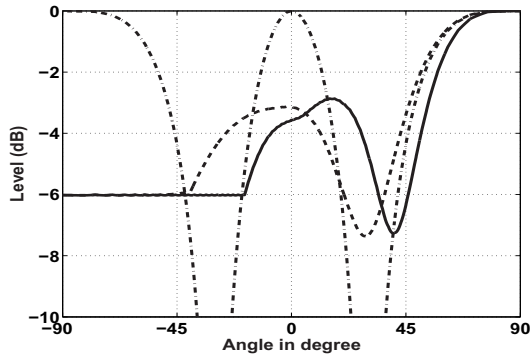


Figure 1: Beampattern of $g(t)$ (solid line) and impulse $g(t)$ (dashed line) arriving at 90° on array 1_2 with 2 elements at distance 2 and of narrowband signal with wavelength λ (dash-dotted)

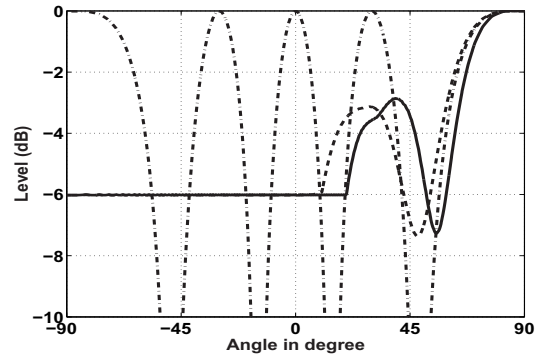


Figure 2: Beampattern of $g(t)$ (solid line) and impulse $g(t)$ (dashed line) arriving at 90° on array 2_2 with 2 elements at distance 2 and of narrowband signal with wavelength λ (dash-dotted)

4. SIMULATION RESULTS

In order to give examples for typical UWB signals, we will evaluate representative beampatterns by numerical simulations. Most often found in the literature is the twice differentiated Gaussian impulse

$$g(t) = (1 - 16 (t/\Delta T)^2) e^{-8 (t/\Delta T)^2}, \quad (14)$$

where the nominal duration ΔT is set to $2 * 10^{-10}$ s, leading to a -3 dB bandwidth from 5 GHz to 11.5 GHz, and an alternate UWB waveform [2]

$$g(t) = \frac{1}{1 - \epsilon} (e^{-4 (t/\Delta T)^2} - \epsilon e^{-4 (\epsilon t/\Delta T)^2}), \quad (15)$$

where the nominal duration ΔT is set to $2.5 * 10^{-10}$ s and the scaling parameter ϵ to 1.5, leading to a -3 dB bandwidth from 3.4 GHz to 8 GHz. The wavelength of the corresponding sinewave is chosen according to a nominal center frequency of 6.85 GHz. Two typical array configurations with different number of antennas are considered throughout this section:

- Array 1_2 has 2 elements at distance 2
- Array 2_2 has 2 elements at distance 2
- Array 1_4 has 4 elements at distance 2
- Array 2_4 has 4 elements at distance 2

Note that in the narrowband case, grating lobes will appear in the beampattern for all scenarios. In figures 1-7, $BP(\theta, \phi)$ is shown for signals arriving at 90° , and the beampattern corresponding to $g(t)$, $g(t)$ whereas in figures 1-4 a sinewave of frequency 6.85 GHz is plotted in the same figure for comparison. It is observed that the mainlobe width for impulse beamforming is approximately the same as for the sinewave with corresponding virtual center frequency. Figures 1 to 7 show the striking feature of impulse beamforming namely the mitigation of grating lobes and the appearance of a fixed sidelobe level. In figures 5 and 6, a Hamming weighting, which is traditionally used in the narrowband case for sidelobe reduction, is applied to the arrays, and in figure 7, the result of applying a bandstop filter with stopband from 6 to 7 GHz in the first and last beamformer channel and a bandpass filter with frequency band from 6 to 7 GHz in the other channels is shown. The result predicted by section 3 can be clearly observed, and the fixed sidelobe level for the unequally weighted / prefiltered array is remarkably higher than for the unweighted / filtered case.

5. CONCLUSION

Interesting results for ideal UWB beampattern have been presented, as the absence of grating lobes and the appearance of a fixed sidelobe level together with the unusual fact that unequal prefiltering or

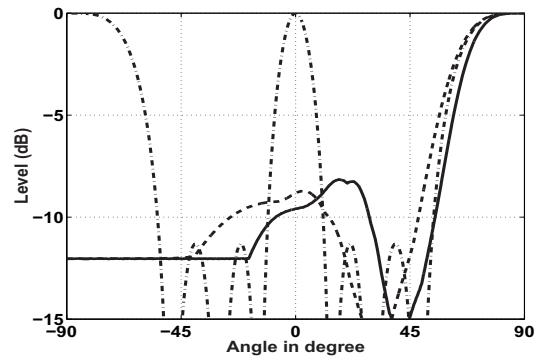


Figure 3: Beampattern of $g(t)$ (solid line) and impulse $g(t)$ (dashed line) arriving at 90° on array 1_4 with 4 elements at distance 2 and of narrowband signal with wavelength λ (dash-dotted)

weighting of the array antennas leads to an *increase* of the sidelobe level. The simulations underline the validity of these unfamiliar results. This means that UWB impulse beamforming is clearly different from narrowband beamforming.

6. APPENDIX

6.1 Appendix 1: Mathematical notations

In the following, a real- or complex- valued signal $s(t)$ defined on the real line \mathbb{R} will be called of *finite duration* with duration T , if it vanishes outside the interval $[-T/2, T/2]$. The *Fourier transform (spectrum)* of a signal $s(t)$ is denoted by

$$S(f) = \int_{-\infty}^{\infty} s(t) e^{-j2\pi f t} dt, \quad (f \in \mathbb{R}).$$

Further, the *energy* of a signal with finite duration is given by

$$E_s = \int_{-T/2}^{T/2} |s(t)|^2 dt = \int_{-\infty}^{\infty} |s(t)|^2 dt,$$

where the formal extension of the integration limit is for convenience.

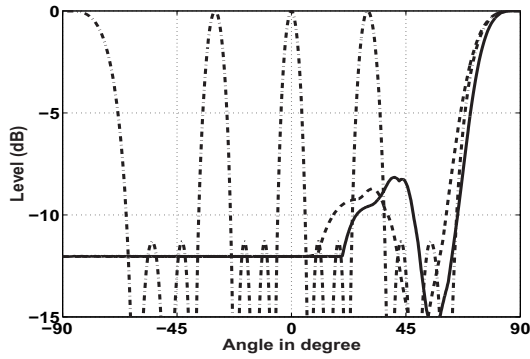


Figure 4: Beampattern of $g(t)$ (solid line) and impulse $g(t)$ (dashed line) arriving at 90° on array 2_4 with 4 elements at distance 2 and of narrowband signal with wavelength (dash-dotted)

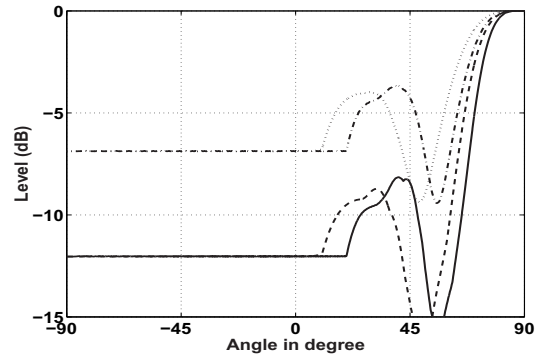


Figure 6: Beampattern of $g(t)$ (solid line) and impulse $g(t)$ (dashed line) arriving at 90° on array 2_4 with 4 elements at distance and of $g(t)$ (dash-dotted line) and impulse $g(t)$ (dotted line) on array 1 with Hamming shading

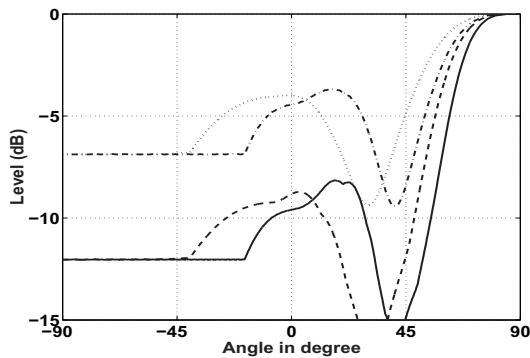


Figure 5: Beampattern of $g(t)$ (solid line) and impulse $g(t)$ (dashed line) arriving at 90° on array 1_4 with 4 elements at distance and of $g(t)$ (dash-dotted line) and impulse $g(t)$ (dotted line) on array 1 with Hamming shading

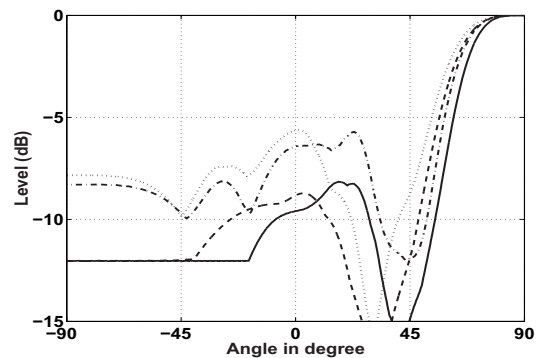


Figure 7: Beampattern of $g(t)$ (solid line) and impulse $g(t)$ (dashed line) arriving at 90° on array 1_4 with 4 elements at distance and of $g(t)$ (dash-dotted line) and impulse $g(t)$ (dotted line) on array 1 with different prefilters

6.2 Appendix 2

We use the frequency domain formulation for the calculations. The maximum value of the beampattern can then be upper bounded by

$$\begin{aligned}
 |\text{BP}(\cdot, \cdot)|^2 &= \left| \int_{-}^{N-1} |h_n S(f)|^2 df \right| \\
 &= \int_{-}^{N-1} |S(f)|^2 df \sum_{n=0}^{N-1} |h_n|^2 \\
 &\leq E_s \sum_{n=0}^{N-1} |h_n|^2 \sum_{n=0}^{N-1} 1 \\
 &= E_s N \sum_{n=0}^{N-1} |h_n|^2,
 \end{aligned} \tag{16}$$

where (16) results from the Cauchy sum inequality [4] and where equality holds if and only if for all n

$$h_n = \cdot, \in \mathbb{C}. \tag{17}$$

Hence, the maximum mainlobe level is obtained if all the h_n are equal; then

$$\text{BP}(\cdot, \cdot)^2 = N^2 h_1 E_s = N^2 \max_n h_n E_s.$$

It can be easily proven that for this case, the ratio in (13) simplifies to the maximum value N .

REFERENCES

- [1] Ch. Buchholz and Th. Kaiser, *Is DoA estimation feasible for dense multipath UWB indoor channels?*, Wireless 2004, Calgary, Canada, July 12-14, 2004.
- [2] M. G. Hussain, *Principles of Space-Time Array Processing for Ultrawide-Band Impulse Radar and Radio Communications*, IEEE Trans. on Vehicular Technologies, vol. 51, no. 3, 2002.
- [3] V. Murino, A. Trucco, and A. Tesei, *Beam Pattern Formulation and Analysis for Wide-band Beamforming Systems using Sparse Arrays*, Signal Processing, Vol. 56, 1997.
- [4] A. Papoulis, *Signal Analysis*, McGraw-Hill, 1985.
- [5] S. Ries and Th. Kaiser, *UWB impulse beamforming: it's a different world*, submitted for publication.
- [6] S. Ries and Th. Kaiser, *Towards Beamforming for UWB Signals*, Proc. EUSIPCO 2004, Vienna, Austria, Sept. 2004.
- [7] S. Ries, Th. Kaiser and Ch. Buchholz, *UWB Beamforming and DoA Estimation*, in UWB Communication Systems - A Comprehensive Overview, EURASIP Book Series, to appear 2005.
- [8] B. Steinberg, *Principles of aperture and array system design*, J. Wiley & Sons, 1976.